DOI: 10.1021/ic9001779

Inorganic Chemistry
Article

Assessing the Dependence of ^{51}V A_z Value on the Aromatic Ring Orientation of $V^{IV}O^{2+}$ Pyridine Complexes

Giovanni Micera,[†] Vincent L. Pecoraro,[‡] and Eugenio Garribba*,[†]

[†]*Dipartimento di Chimica, Università di Sassari, Via Vienna 2, I-07100 Sassari, Italy, and*
[‡]*Department of Chemistry, University of Michigan, Ann Arbor, Michigan 48109-1055*

Received January 28, 2009

Characterization of V^{IV} biomolecules relies strongly on electron paramagnetic resonance (EPR) spectroscopy, particularly the application of the additivity relationship of A_z values. It has been shown experimentally that the A_z values of $V^{IV}O^{2+}$ imidazole species have a critical angular dependence. Density-functional theory (DFT) calculations elucidate the dependence of ^{51}V A_z value on the orientation of the aromatic ring in $V^{IV}O^{2+}$ pyridine complexes, following closely the functional dependence observed for $V^{IV}O^{2+}$ imidazole species, [A_z(pyr) = 42.23 + 1.80 × sin(2θ − 90)], with A_z measured in 10^4 cm^{-1}. A DFT re-examination of $V^{IV}O^{2+}$ imidazole complexes gives an equation very similar [A_z(imid) = 42.35 + 2.34 × sin(2θ − 90)] to that experimentally found. These results generalize the application of the additivity relationship for $V^{IV}O^{2+}$ complexes containing aromatic nitrogen ligands such as pyridine or imidazole. The increase of the absolute value of A_z, $|A_z|$, when the dihedral angle θ between the V═O and N_{pyr}−C or N_{imid}−C bonds varies from a parallel to a perpendicular orientation is due to an increase of the d vanadium orbital contribution and to a decrease of the π aromatic system participation in the singly occupied molecular orbital.

Introduction

Vanadium plays a number of roles in biological systems,[1] and in humans its complexes have shown promising activity for the treatment of type II diabetes.[2] Independent of the initial oxidation state, vanadium is transported in the blood as the $V^{IV}O^{2+}$ form.[3,4]

Electron paramagnetic resonance (EPR) spectroscopy has been revealed to be the most powerful tool for the investigation of the electronic structure and geometry of $V^{IV}O^{2+}$ compounds.[5] Usually, the characterization is performed through the application of the additivity relationship, which affirms that the ^{51}V anisotropic hyperfine coupling constant along the z axis (A_z) can be calculated from the sum of the contributions of each equatorial donor.[6,7]

Initial studies used a set value for imidazole binding to V^{IV} in proteins; however, it was later demonstrated that the orientation of equatorial imidazole rings relative to the V═O bond critically influences the A_z values in $V^{IV}O^{2+}$ model complexes.[8] Subsequent evaluation of discrepancies in previously examined biomolecules demonstrated the importance of considering the influence of ring orientation on the predicted A_z values.[8] It was found that the contribution to A_z of the imidazole (A_z(imid)) ranges from 39.8 (parallel orientation of the aromatic ring with respect to the V═O bond) to 45.6 × 10^{-4} cm^{-1} (perpendicular orientation). An equation was proposed, A_z(imid) = 42.72 + 2.96 × sin(2θ − 90), with the dihedral angle θ defined by the V═O and N_{imid}−C bonds, where C is the carbon atom bridging the two imidazole nitrogens. This dependence of the A_z value on the imidazole ring orientation was used to interpret the EPR and electron spin echo envelope modulation spectra of vanadium bromoperoxidase (VBrPO).[8]

* To whom correspondence should be addressed. E-mail: garribba@uniss.it.

(1) (a) Crans, D. C.; Smee, J. J.; Gaidamauskas, E.; Yang, L. *Chem. Rev.* **2004**, *104*, 849–902. (b) Rehder, D. *Bioinorganic Vanadium Chemistry*; Wiley & Sons: Chichester, U. K., 2008.

(2) (a) Thompson, K. H.; Orvig, C. *Coord. Chem. Rev.* **2001**, *219*−*221*, 1033–1053 and references therein. (b) Shechter, Y.; Goldwaser, I.; Mironchik, M.; Fridkin, M.; Gefel, D. *Coord. Chem. Rev.* **2003**, *237*, 3–11 and references therein. (c) Thompson, K. H.; Orvig, C. *J. Inorg. Biochem.* **2006**, *100*, 1925–1935.

(3) (a) Kustin, K. Robinson, W. E. In *Metal Ions in Biological Systems*; Sigel, A., Sigel, H., Eds.; Marcel Dekker: New York, 1995; Vol *31*, pp 511−542. (b) Nielsen, F. H. In *Metal Ions in Biological Systems*; Sigel, A., Sigel, H., Eds.; Marcel Dekker: New York, 1995; Vol *31*, pp 543−573.

(4) (a) Kiss, T.; Jakusch, T.; Hollender, D.; Dörnyei, A. In *Vanadium: the Versatile Metal*; Kustin, K., Costa Pessoa, J., Crans, D. C., Eds.; ACS Symposium Series 974, American Chemical Society: Washington, DC, 2007; pp 323−339. (b) Kiss, T.; Jakusch, T.; Hollender, D.; Dörnyei, A.; Enyedy, E. A; Costa Pessoa, J.; Sakurai, H.; Sanz-Medel, A. *Coord. Chem. Rev.* **2008**, *252*, 1153–1162 and references therein.

(5) Garner, C. D.; Collison, D.; Mabbs, F. E. In *Metal Ions in Biological Systems*; Sigel, A.; Sigel, H., Eds.; Marcel Dekker: New York, 1995; Vol *31*, pp 617−670.

(6) Chasteen, N. D. In *Biological Magnetic Resonance*; Berliner, L. J., Reuben, J., Eds.; Plenum Press: New York, 1981; Vol *3*, pp 53−119.

(7) Smith, T. S.II; LoBrutto, R.; Pecoraro, V. L. *Coord. Chem. Rev.* **2002**, *228*, 1–18.

(8) Smith, T. S.II; Root, C. A.; Kampf, J. W.; Rasmussen, P. G.; Pecoraro, V. L. *J. Am. Chem. Soc.* **2000**, *122*, 767–775.

Published on Web 05/18/2009

Density functional theory (DFT) allows for calculating EPR parameters of transition metal complexes,[9] and more particularly of $V^{IV}O^{2+}$ species.[10−13] Therefore, computational methods may support the additivity relationship in the characterization of such compounds. By using DFT calculations, Saladino and Larsen theoretically confirmed the orientation dependence of A_z(imid) on the dihedral angle θ.[14] Nevertheless, the resultant equation, $A_z(\text{imid}) = 27.31 + 2.26 \times \sin(2\theta - 90)$, although reproducing the covered range well (4.5 calculated vs 5.9×10^{-4} cm^{-1} experimental) is centered 36.1% lower than the experimentally found value. Recently, some of us achieved consistent success in the prediction of the ^{51}V hyperfine coupling constants with respect to the previous results, calculating A_z for 22 representative $V^{IV}O^{2+}$ complexes having different charges, geometries, and coordination modes at the BHandHLYP/6-311g(d,p) level of theory with a mean deviation of 2.7% from the experimental values.[15]

Recognizing that DFT is able to calculate A_z for $V^{IV}O^{2+}$ species, we next hoped to evaluate through DFT methods whether the same angular dependence contribution to A_z was observed in complexes containing an alternative aromatic ring with a nitrogen donor, pyridine. Herein, we assess the hypothesis that the A_z value is susceptible to the variations of the aromatic ring nitrogen-containing ligands and re-evaluate the calculation for the biologically critical imidazole ligand.

Computational Section

DFT Calculations. All of the calculations presented were performed using the Gaussian 03 program (revision C.02)[16] and DFT methods.[17] The hybrid exchange-correlation functional B3LYP,[18,19] used in the optmization of the $V^{IV}O^{2+}$ structures, and the half-and-half functional BHandHLYP, used in the calculation of the EPR parameters, were incorporated in the Gaussian 03 software.

The geometries of $[VO(pyr)(H_2O)_3]^{2+}$ and $[VO(imid)(H_2O)_3]^{2+}$ complexes were first preoptimized at the B3LYP/sto-3g level and further optimized as a function of the dihedral angle θ at the B3LYP/6-311g level of theory. Analogous calculations were performed for the optimization of $[VO(H_2O)_4]^{2+}$. For all of the structures, minima were verified through frequency calculations. The optimized geometries were used to calculate the ^{51}V hyperfine coupling constants (A_{iso}, A_x, A_y, and A_z) at the BHandHLYP/6-311g(d,p) level.

The analysis of molecular orbital (MO) composition in terms of atomic orbitals or groups of atoms was performed using the AOMix program.[20]

Theory Background. Wüthrich has first pointed out that the hyperfine coupling constant (A value) between the unpaired electron and the nucleus of ^{51}V in tetragonal complexes of the $V^{IV}O^{2+}$ ion is particularly sensitive to the donors coordinated in its equatorial plane.[21] Subsequently, Chasteen developed this idea and introduced the additivity relationship, an empirical rule affirming that the values of the ^{51}V anisotropic hyperfine coupling constant along the z axis measured for a $V^{IV}O^{2+}$ complex (as a polycrystalline powder or a frozen sample) can be calculated from the sum of the contributions of each equatorial donor function:[6]

$$A_z^{\text{calcd}} = \sum_{i=1}^{4} A_z(\text{donor } i) = A_z(\text{donor 1}) + A_z(\text{donor 2}) + A_z(\text{donor 3}) + A_z(\text{donor 4}) \quad (1)$$

Initially, a set value for the contribution of the aromatic nitrogen was used to calculate A_z for $V^{IV}O^{2+}$ imidazole complexes. However, it was shown that significant errors in the prediction of A_z would arise, and a wrong structure would be deduced, if account was not made of the relative orientation of the imidazole ring with respect to the V=O vector.[8] Additions or corrections about the contribution of CO, Cl^- and SCN^-, COO^-, and N_{imine} have appeared over the past few years in the literature.[22]

The $V^{IV}O^{2+}$ ion has a d^1 electronic configuration with one unpaired electron. The hyperfine coupling constant in an EPR spectrum arises from the interaction between the spin angular momentum of the electron ($S = 1/2$) and the spin angular momentum of the ^{51}V nucleus ($I = 7/2$, 99.8% natural abundance). In the first-order approximation, the vanadium hyperfine coupling tensor **A** has one isotropic contribution deriving from the Fermi contact (A_{iso}) and another from the anisotropic or dipolar hyperfine interaction, expressed by tensor **T**.[9,11,12,14,23]

$$\mathbf{A} = A_{iso}\mathbf{1} + \mathbf{T} \quad (2)$$

with **1** the unit tensor.

(9) *Calculation of NMR and EPR Parameters. Theory and Applications*; Kaupp, M., Buhl, M., Malkin, V. G., Eds.; Wiley-VCH: Weinheim, Germany, 2004.
(10) Munzarová, M. L.; Kaupp, M. *J. Phys. Chem. B* **2001**, *105*, 12644–12652 and references therein.
(11) (a) Saladino, A. C.; Larsen, S. C. *J. Phys. Chem. A* **2003**, *107*, 1872–1878. (b) Saladino, A. C.; Larsen, S. C. *Catal. Today* **2005**, *105*, 122–133 and references therein.
(12) Aznar, C. P.; Deligiannakis, Y.; Tolis, E. J.; Kabanos, T. A.; Brynda, M.; Britt, R. D. *J. Phys. Chem. A* **2004**, *108*, 4310–4321.
(13) Neese, F. *Coord. Chem. Rev.* **2009**, *253*, 526–563.
(14) Saladino, A. C.; Larsen, S. C. *J. Phys. Chem. A* **2002**, *106*, 10444–10451.
(15) Micera, G.; Garribba, E. *Dalton Trans.* **2009**, 1914–1918.
(16) Frisch, M. J..; Trucks, G. W.; Schlegel, H. B.; Scuseria, G. E.; Robb, M. A.; Cheeseman, J. R.; Montgomery, J. A., Jr.; Vreven, T.; Kudin, K. N.; Burant, J. C.; Millam, J. M.; Iyengar, S. S.; Tomasi, J.; Barone, V.; Mennucci, B.; Cossi, M.; Scalmani, G.; Rega, N.; Petersson, G. A.; Nakatsuji, H.; Hada, M.; Ehara, M.; Toyota, K.; Fukuda, R.; Hasegawa, J.; Ishida, M.; Nakajima, T.; Honda, Y.; Kitao, O.; Nakai, H.; Klene, M.; Li, X.; Knox, J. E.; Hratchian, H. P.; Cross, J. B.; Adamo, C.; Jaramillo, J.; Gomperts, R.; Stratmann, R. E.; Yazyev, O.; Austin, A. J.; Cammi, R.; Pomelli, C.; Ochterski, J. W.; Ayala, P. Y.; Morokuma, K.; Voth, G. A.; Salvador, P.; Dannenberg, J. J.; Zakrzewski, V. G.; Dapprich, S.; Daniels, A. D.; Strain, M. C.; Farkas, O.; Malick, D. K.; Rabuck, A. D.; Raghavachari, K.; Foresman, J. B.; Ortiz, J. V.; Cui, Q.; Baboul, A. G.; Clifford, S.; Cioslowski, J.; Stefanov, B. B.; Liu, G.; Liashenko, A.; Piskorz, P.; Komaromi, I.; Martin, R. L.; Fox, D. J.; Keith, T.; Al-Laham, M. A.; Peng, C. Y.; Nanayakkara, A.; Challacombe, M.; Gill, P. M. W.; Johnson, B.; Chen, W.; Wong, M. W.; Gonzalez, C.; Pople, J. A. *Gaussian 03*, revision C.02; Gaussian, Inc.: Wallingford CT, 2004.
(17) Parr, R. G.; Yang, W. *Density-Functional Theory of Atoms and Molecules*; Oxford University Press: Oxford, U. K., 1989.
(18) Becke, A. D. *J. Chem. Phys.* **1993**, *98*, 5648–5652.
(19) Lee, C.; Yang, W.; Parr, R. G. *Phys. Rev. B* **1988**, *37*, 785–789.
(20) (a) Gorelsky, S. I. *AOMix: Program for Molecular Orbital Analysis*; University of Ottawa: Ontario, Canada, 2009; http://www.sg-chem.net (accessed Mar 2009). (b) Gorelsky, S. I.; Lever, A. B. P. *J. Organomet. Chem.* **2001**, *635*, 187–196.
(21) Wüthrich, K. *Helv. Chim. Acta* **1965**, *48*, 1012–1017.
(22) (a) Hamstra, B. J.; Houseman, A. P. L.; Colpas, G. J.; Kampf, J. W.; LoBrutto, R.; Frasch, W. D.; Pecoraro, V. L. *Inorg. Chem.* **1997**, *36*, 4866–4874. (b) Tolis, E. J.; Teberekidis, V. I.; Raptopoulou, C. P.; Terzis, A.; Sigalas, M.; Deligiannakis, Y.; Kabanos, T. A. *Chem.—Eur. J.* **2001**, *7*, 2698–2710. (c) Jakusch, T.; Buglyó, P.; Tomaz, A. I.; Costa Pessoa, J.; Kiss, T. *Inorg. Chim. Acta* **2002**, *339*, 119–128. (d) Garribba, E.; Lodyga-Chruscinska, E.; Micera, G.; Panzanelli, A.; Sanna, D. *Eur. J. Inorg. Chem.* **2005**, 1369–1382 and references therein.
(23) (a) Drago, R. S. *Physical Methods in Chemistry*; Saunders: Philadelphia, 1977. (b) Wertz, J. E.; Bolton, J. R. *Electron Spin Resonance: Elementary Theory and Practical Applications*; Chapman and Hall: New York, 1986. (c) Mabbs, F. E.; Collison, D. *Electron Paramagnetic Resonance of d-Transition Metal Compounds*; Elsevier: Amsterdam, 1992.

A_{iso} and the components T_{jk} of the tensor **T** are given by the following equations:

$$A_{iso} = \frac{4\pi}{3} g_e g_N \beta_e \beta_N \langle S_z \rangle^{-1} \rho^{\alpha-\beta} \quad (3)$$

$$T_{jk} = \frac{1}{2} g_e g_N \beta_e \beta_N \langle S_z \rangle^{-1} \sum_{k,l} P_{k,l}^{\alpha-\beta} \langle \Phi_k | \frac{r^2 \delta_{jk} - 3 r_j r_k}{r^5} | \Phi_l \rangle \quad (4)$$

where g_e is the g value of the free electron (2.0023), g_N is the nuclear g value, β_e is the Bohr magneton, β_N is the nuclear magneton, $\langle S_z \rangle$ is the expectation value of the electronic spin on the z axis, $\rho^{\alpha-\beta}$ is the spin density at the nucleus, $P_{k,l}^{\alpha-\beta}$ is the spin density matrix, and **r** the distance between the unpaired electron and the nucleus. If T_x, T_y, and T_z are the elements of the tensor **T** in the diagonalized form, the values of the ^{51}V anisotropic hyperfine coupling constants along the x, y, and z axes are

$$A_x = A_{iso} + T_x \quad (5)$$

$$A_y = A_{iso} + T_y \quad (6)$$

$$A_z = A_{iso} + T_z \quad (7)$$

A_{iso} and A_z values (as well as A_x and A_y) are negative, but in the literature, these are usually reported as absolute values. In order to avoid confusion, the absolute values of A_{iso} and A_z are indicated in the manuscript as $|A_{iso}|$ and $|A_z|$.

$V^{IV}O^{2+}$ Complexes and EPR Parameters. All of the structural details and the EPR parameters reported in the text were taken from refs 8, 22b, 24−34.

Results and Discussion

The calculations were performed on $[VO(pyr)(H_2O)_3]^{2+}$ and $[VO(imid)(H_2O)_3]^{2+}$, varying the dihedral angle θ between the V=O and N_{pyr}−C or N_{imid}−C bonds from 0 to 180°. The optimized structures of $[VO(pyr)(H_2O)_3]^{2+}$ for a parallel and perpendicular orientation of the aromatic ring with respect to the V=O group are shown in Figure 1.

In Table 1 are reported the results obtained for pyridine for θ in the range 0−90°; the complete list of the data is presented in Table S1 of the Supporting Information. The pyridine nitrogen contribution to A_z (A_z(pyr)) for each value of θ is determined by subtracting from the absolute value of A_z calculated for $[VO(pyr)(H_2O)_3]^{2+}$ (Table 1) the contribution of three water molecules:

$$A_z(pyr) = [|A_z|(VO(pyr)(H_2O)_3^{2+}) - 3A_z(H_2O)] \quad (8)$$

The contribution of an equatorial water, (A_z(H_2O)), of 46.9 × 10^{-4} cm^{-1} was derived from $|A_z|$ calculated for $[VO(H_2O)_4]^{2+}$, 187.6 × 10^{-4} cm^{-1}.

From an analysis of the data emerges the observation that both the absolute values of A_{iso} and T_z increase from 0 to 90° (Table 1), that is, by going from a parallel to a perpendicular orientation of the aromatic ring with respect to the V=O bond, and decrease from 90 to 180° (Table S1 of the Supporting Information). The greater contribution to A_z comes from A_{iso}, which ranges from −112.7 to −116.2 × 10^{-4} cm^{-1}, rather than from T_z, which changes from −68.3 to −68.6 × 10^{-4} cm^{-1}. The dependence of the A_z(pyr) value on the dihedral angle θ is displayed in Figure 2.

A least-squares fit of the calculated A_z(pyr) values yields a curve of equation

$$A_z(pyr) = 42.23 + 1.80 \times \sin(2\theta - 90) \quad (9)$$

with A_z measured in units of 10^{-4} cm^{-1}.

These results for pyridine complexes support the general hypothesis for aromatic amines, previously forwarded specifically for imidazole, that the functional dependence can be attributed to the overlap between the vanadium d_{xy} bearing the unpaired electron and the aromatic π orbital, that in turn depends on the dihedral angle θ.[8]

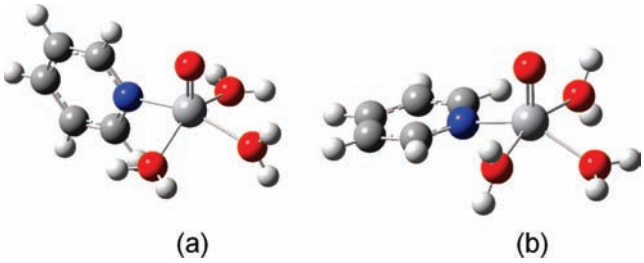

Figure 1. Optimized structure of $[VO(pyr)(H_2O)_3]^{2+}$ at the B3LYP/6-311g level of theory with a value of the dihedral angle θ between the V=O and N−C bonds of the aromatic ring of (a) 0° (parallel orientation) and (b) 90° (perpendicular orientation).

Table 1. Calculated EPR Parameters at BHandHLYP/6-311g(d,p) for the $[VO(pyr)(H_2O)_3]^{2+}$ Complex and Contribution of a Pyridine Nitrogen to A_z (A_z(pyr))[a,b]

dihedral angle	A_{iso}	T_x	T_y	T_z	A_x	A_y	A_z	A_z(pyr)
0°	−112.7	33.6	34.8	−68.3	−79.2	−78.0	−181.1	40.4
10°	−112.9	33.6	34.8	−68.3	−79.3	−78.1	−181.3	40.6
20°	−113.2	33.6	34.7	−68.3	−79.6	−78.4	−181.5	40.8
30°	−113.6	33.6	34.7	−68.3	−80.0	−78.9	−181.9	41.3
40°	−114.2	33.7	34.6	−68.3	−80.6	−79.6	−182.5	41.8
50°	−114.8	33.7	34.6	−68.3	−81.1	−80.2	−183.1	42.4
60°	−115.4	33.8	34.6	−68.3	−81.7	−80.9	−183.8	43.1
70°	−115.9	34.0	34.5	−68.5	−81.9	−81.4	−184.3	43.7
80°	−116.0	33.9	34.6	−68.5	−82.1	−81.4	−184.5	43.9
90°	−116.2	34.0	34.6	−68.6	−82.2	−81.5	−184.7	44.1

[a] All of the parameters are measured in 10^{-4} cm^{-1}. [b] The contribution of a H_2O molecule, 46.9 × 10^{-4} cm^{-1}, was derived from $|A_z|$ calculated for $[VO(H_2O)_4]^{2+}$, 187.6 × 10^{-4} cm^{-1}.

(24) Hanson, G. R.; Kabanos, T. A.; Keramidas, A. D.; Mentzafos, D. *Inorg. Chem.* **1992**, *31*, 2587–2594.
(25) Kabanos, T. A.; Keramidas, A. D.; Papaioannou, A. B.; Terzis, A. *Chem. Comm.* **1993**, 643–645.
(26) Cavaco, I.; Costa Pessoa, J.; Costa, D.; Duarte, M. T.; Gillard, R. D.; Matias, P. *J. Chem. Soc., Dalton Trans.* **1994**, 149–157.
(27) Tasiopoulos, A. J.; Vlahos, A. T.; Keramidas, A. D.; Kabanos, T. A.; Deligiannakis, Y. G.; Raptopoulou, C. P.; Terzis, A. *Angew. Chem., Int. Ed.* **1996**, *35*, 2531–2533.
(28) Gätjens, J.; Maier, B.; Kiss, T.; Nagy, E. M.; Buglyó, P.; Sakurai, H.; Kawabe, K.; Rehder, D. *Chem.—Eur. J.* **2003**, *9*, 4924–4935.
(29) Dean, N. S.; Bartley, S. L.; Streib, W. E.; Lobkovsky, E. B.; Christou, G. *Inorg. Chem.* **1995**, *34*, 1608–1616.
(30) Samanta, S.; Ghosh, D.; Mukhopadhyay, S.; Endo, A.; Weakley, T. J. R.; Chaudhury, M. *Inorg. Chem.* **2003**, *42*, 1508–1517.
(31) Calviou, L. J.; Arber, J. M.; Collison, D.; Garner, C. D.; Clegg, W. *Chem. Comm.* **1992**, 654–656.
(32) Cornman, C. R.; Kampf, J.; Lah, M. S.; Pecoraro, V. L. *Inorg. Chem.* **1992**, *31*, 2035–2043.
(33) Less, G. B.; Ockwig, N. W.; Rasmussen, P. G.; Smith, G. D.; Keller, L. M.; Drach, J. C. *Inorg. Chem.* **2006**, *45*, 7105–7110.
(34) Crans, D. C.; Keramidas, A. D.; Amin, S. S.; Anderson, O. P.; Miller, S. M. *J. Chem. Soc., Dalton Trans.* **1997**, 2799–2812.

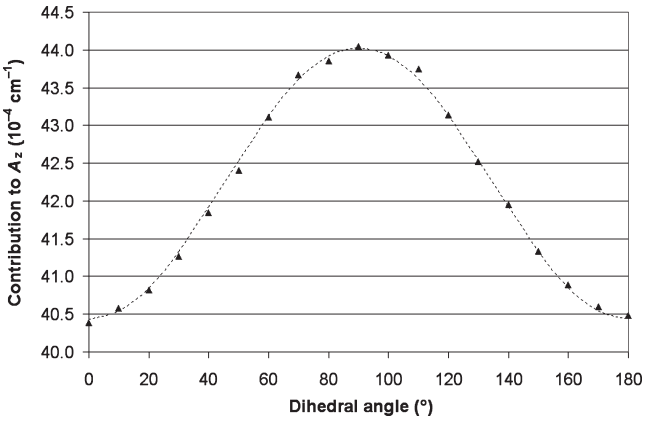

Figure 2. Contribution of a pyridine nitrogen to A_z (A_z(pyr)) as a function of the dihedral angle θ between the V=O and N−C bonds of the aromatic ring. The triangles represent the calculated values, measured in 10^{-4} cm^{-1}, and the dotted line the equation fitting the points A_z(pyr) = 42.23 + 1.80 × sin(2θ − 90). The R^2 value for fitting is 0.9978.

A further analysis of the data suggests that the observed dependence of A_z(pyr) on θ rises from the angular variation of the $|A_{iso}|$ value, which follows the same functional relationship $A + B \times \sin(2\theta - 90)$:

$$|A_{iso}|(VO(pyr)(H_2O)_3^{2+}) = 114.51 + 1.71 \times \sin(2\theta - 90) \quad (10)$$

Figure 3 shows the $|A_{iso}|$ for the $[VO(pyr)(H_2O)_3]^{2+}$ complex as a function of the dihedral angle θ between the V=O and N−C bonds of the aromatic ring.

Analogous simulations on $[VO(imid)(H_2O)_3]^{2+}$ allow one to obtain a similar trend. The parameters obtained from the DFT simulations of $[VO(imid)(H_2O)_3]^{2+}$ for the dihedral angle θ in the range 0−90° are listed in Table 2. The complete results are reported in Table S3 of the Supporting Information.

The contribution to A_z of an imidazole nitrogen (A_z(imid)) follows a functional dependence similar to that found for pyridine:

$$A_z(imid) = 42.35 + 2.34 \times \sin(2\theta - 90) \quad (11)$$

Moreover, for imidazole too, such a dependence comes from the variation of $|A_{iso}|$ with the dihedral angle θ:

$$|A_{iso}|(VO(imid)(H_2O)_3^{2+}) = 114.63 + 2.27 \times \sin(2\theta - 90) \quad (12)$$

In Figure 4, the data here obtained for A_z(imid), together with the experimental and simulated curves reported by Smith et al. and Saladino and Larsen,[8,14] are represented.

A comparison of the results obtained in this work for pyrdine and imidazole indicates that the mean value of A_z(pyr) is slightly lower (42.23 vs 42.35 × 10^{-4} cm^{-1}), and that the total variation of A_z(pyr) is smaller (3.60 vs 4.68 × 10^{-4} cm^{-1}). Our data reproduce the experimental values, both in the mean value and in the range covered by A_z(imid);[8] they improve upon the previous calculation of Saladino and Larsen,[14] which on one hand correctly predicted the total range spanned by A_z(imid) but, on the other, provided a significantly lower mean value of the sine function (27.31 vs 42.35 calculated in this work and 42.72 × 10^{-4} cm^{-1} by Smith et al.[8]).

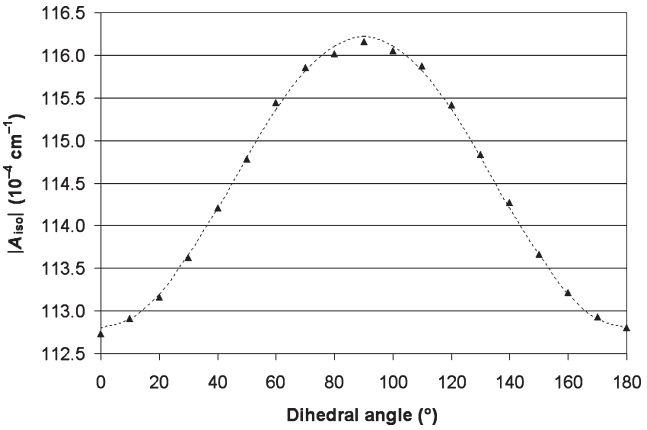

Figure 3. $|A_{iso}|$ for the $[VO(pyr)(H_2O)_3]^{2+}$ complex as a function of the dihedral angle θ between the V=O and N−C bonds of the aromatic ring. The triangles represent the calculated values, measured in 10^{-4} cm^{-1}, and the dotted line the equation fitting the points $|A_{iso}|$ = 114.51 + 1.71 × sin (2θ − 90). The R^2 value for fitting is 0.9985.

Table 2. Calculated EPR Parameters at BHandHLYP/6-311g(d,p) for the $[VO(imid)(H_2O)_3]^{2+}$ Complex and Contribution of an Imidazole Nitrogen to A_z (A_z(imid))[a,b]

dihedral angle	A_{iso}	T_x	T_y	T_z	A_x	A_y	A_z	A_z (imid)
0°	−112.3	33.7	34.8	−68.4	−78.6	−77.5	−180.7	40.0
10°	−112.5	33.6	34.8	−68.4	−78.8	−77.7	−180.9	40.2
20°	−112.9	33.6	34.8	−68.4	−79.3	−78.1	−181.3	40.6
30°	−113.7	33.6	34.7	−68.3	−80.2	−79.0	−182.1	41.4
40°	−114.3	33.6	34.6	−68.3	−80.7	−79.7	−182.6	41.9
50°	−114.9	33.8	34.5	−68.3	−81.2	−80.4	−183.2	42.5
60°	−115.7	33.9	34.4	−68.3	−81.8	−81.3	−184.1	43.4
70°	−116.5	33.9	34.6	−68.5	−82.6	−81.9	−185.0	44.4
80°	−116.8	33.8	34.7	−68.5	−83.0	−82.1	−185.4	44.7
90°	−117.0	33.8	34.7	−68.5	−83.2	−82.2	−185.5	44.8

[a] All of the parameters measured in 10^{-4} cm^{-1}. [b] The contribution of a H_2O molecule, 46.9 × 10^{-4} cm^{-1}, was derived from $|A_z|$ calculated for $[VO(H_2O)_4]^{2+}$, 187.6 × 10^{-4} cm^{-1}.

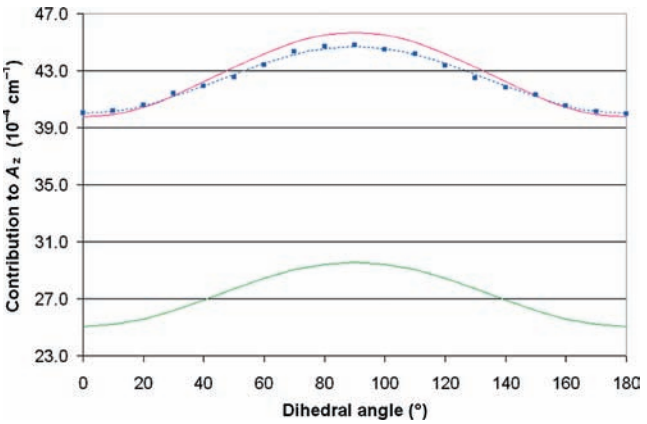

Figure 4. Contribution of an imidazole nitrogen to A_z (A_z(imid)) as a function of the dihedral angle θ between the V=O and N−C bonds of the aromatic ring (as defined in the text). The blue squares represent the values calculated in this work and the blue dotted line the equation fitting the points: A_z(imid) = 42.35 + 2.34 × sin(2θ − 90). The R^2 value for fitting is 0.9940. The full pink line displays the equation of ref 8, A_z(imid) = 42.72 + 2.96 × sin(2θ − 90), and the full green line represents the equation of ref 14, A_z(imid) = 27.31 + 2.26 × sin(2θ − 90). For all of the curves, A_z(imid) is measured in 10^{-4} cm^{-1}.

Table 3. Experimental and Calculated A_z Values for $V^{IV}O^{2+}$ Pyridine and Imidazole Complexes[a]

complex[b]	donor set	θ[c]	θ[d]	$A_z^{calcd\ e,f}$	$A_z^{calcd\ e,g}$	$A_z^{calcd\ e,h}$	A_z^{exptl}	ref
[VO(pycac)]	N_{pyr}, N_{amide}^-, NH, RO^-	77.1		151.6	154.8		151.4	24
$[VO(hypyb)]^-$	N_{pyr}, N_{amide}^-, N_{amide}^-, O_{ar}^-	76.9		156.2	159.3		156.1	25
$[VO(SalGly)(pyr)_2]$	COO^-, N_{imine}, O_{ar}^-; N_{pyr}; N_{pyr}^{ax}	86.2		163.3	166.6		167.3	26
[VO(Sal-L-Ala)(bipy)]	COO^-, N_{imine}, O_{ar}^-; N_{pyr}, N_{pyr}^{ax}	2.1		163.3	163.0		163.8	26
$[VO(dipic)(HDMCI)]^-$	COO^-, N_{pyr}, COO^-; N_{imid}, COO^{-ax}	91.5		164.7	168.1		167.0	8
[VO(capcah)Cl]	N_{pyr}, N_{amide}^-, N_{imine}, Cl^-; N_{pyr}^{ax}	88.1		162.0	165.3		163.0	22b
$[VO(mpg)(phen)]^-$	COO^-, N_{amide}^-, RS^-; N_{phen}, N_{phen}^{ax}	0.4		153.0	152.7		151.1	27
cis-$[VO(5MeOpic)_2(H_2O)]$	N_{pyr}, COO^-; N_{pyr}, COO^{-ax}; H_2O	8.2, 64.1		169.1	171.5		168	28
$[VO(SPh)_3(Me_2bipy)]^-$	S_{ar}^-; S_{ar}^-; S_{ar}^-; N_{pyr}, N_{pyr}^{ax}	3.9		146.6	146.3		148.6	29
$[VO(mdtc)(N\text{-MeIm})_2]$	O_{ar}^-, N_{imine}^{ax}, RS^-; N_{imid}; N_{imid}		170.3, −170.1	150.7	151.1	121.2	158	30
$[VO(1\text{-VinIm})_4]^{2+}$	N_{imid}; N_{imid}; N_{imid}; N_{imid}		155.6, −13.9	161.7	162.2	102.3	162	31
$[VO(SalimH)_2]$	O_{ar}^-, N_{imine}, N_{imid}; O_{ar}^{-ax}, N_{imine}		58.7	166.2	165.5	150.5	159.6	32
[VO(SalimRH)(acac)]	O_{ar}^-, NH, N_{imid}; O_{acac}, O_{acac}^{ax}		96.4	167.1	166.1	151.0	162.3	8
cis-$[VO(HMDCI)_2(H_2O)]$	N_{imid}, COO^-; N_{imid}, COO^{-ax}; H_2O		6.4, 78.7	173.0	172.3	142.2	171.0	8
$[VO(H_2O)(acac)(HMDCI)]$	O_{acac}, O_{acac}; N_{imid}, COO^{-ax}; H_2O		1.3	170.4	170.6	155.6	170.0	8
$[VO(capcah)(imid)]^+$	N_{pyr}, N_{amide}^-, N_{imine}, N_{imid}; N_{pyr}^{ax}	78.5	27.1	156.0	159.2	141.0	158.0	22b
cis-$[VO(DCIpy)_2(H_2O)]$	N_{imid}, N_{pyr}; N_{imid}, N_{pyr}^{ax}; H_2O	104.7	175.7, −110.7	171.0	173.5	140.4	170	33
$[VO(bmida)(H_2O)]$	N_{imid}, COO^-, COO^-, N^{ax}; H_2O		−172.9	169.7	169.9	154.9	170.8	34

[a] Absolute values of A_z are measured in 10^{-4} cm^{-1}. [b] pycac, *N*-(2-(4-oxopent-2-en-2-ylamino)phenyl)pyridine-2-carboxamidato; hypyb, 1-(2-hydroxybenzamido)-2-(2-pyridinecarboxamido)benzenato; SalGly, *N*-salicylideneglycinato; pyr, pyridine; Sal-L-Ala, *N*-salicylidene-L-alaninato; bipy, 2,2′-bipyridine; dipic, pyridine-2,6-dicarboxylato; HDMCI, 1-methyl-5-carboxyimidazole-4-carboxylato; capcah, *N*-(2-((2-pyridylmethyl)amino) phenyl)pyridine-2-carboxamidato; mpg, *N*-(2-mercaptopropionyl)-glycinato; phen, 1,10-phenanthroline; MeOpic, 5-(methoxycarbonyl)pyridine-2-carboxylato; SPh, phenylthiolato; Me_2bipy, 4,4′-dimethyl-2,2′-bipyridine; mdtc, S-methyl-3-((5-bromo-2-hydroxyphenyl)methyl)dithiocarbazato; *N*-MeIm, *N*-methylimidazole; 1-VinIm, 1-vinylimidazole; salimH, 4-(2-(salicylideneamino)ethyl)imidazole; SalimRH, *N*-(*o*-hydroxyphenyl)istamine; acac, acetylacetonato; imid, imidazole; DCIpy, 2-(2-pyridyl)-4,5-dicyanoimidazolato; bmida, *N*-(benzimidazol-2-ylmethyl)iminodiacetato. [c] Mean value of the two dihedral angles between the V=O and the two N−C bonds of the equatorial pyridine ring. [d] Dihedral angle between the V=O and N−C bonds, where C is the carbon atom bridging the two nitrogens, of the equatorial imidazole ring. [e] Contributions of the all the donors taken from ref 22d, except for O_{acac} (42.5×10^{-4} cm^{-1}) taken from ref 8. [f] Contribution of N_{imid} calculated with the equation reported in ref 8, $A_z(imid) = 42.72 + 2.96 \times \sin(2\theta - 90)$, and of N_{pyr}, considered constant (40.7×10^{-4} cm^{-1}, ref 6). [g] Contribution of N_{imid} and N_{pyr} calculated with the eqs 9 and 11. [h] Contribution of N_{imid} calculated with the equation reported in ref 14, $A_z(imid) = 27.31 + 2.26 \times \sin(2\theta - 90)$, and of N_{pyr}, considered constant (40.7×10^{-4} cm^{-1}, ref 6).

The subsequent step was the application of the results obtained here to the $V^{IV}O^{2+}$ complexes containing at least one $V-N_{pyr}$ or $V-N_{imid}$ bond. A search in the literature for mononuclear structures with such bonds yielded 120 hits in the first and 18 in the second case;[35] nevertheless, the EPR parameters are reported for only 35 compounds with a $V-N_{pyr}$ bond and for 14 with a $V-N_{imid}$ bond. The results of the analysis for some representative complexes are listed in Table 3, and in Tables S2 and S4 of the Supporting Information. An examination of the Table 3 shows that the A_z values predicted for $V^{IV}O^{2+}$ pyridine complexes using eq 9 are in good agreement with the experimental ones and, often, are closer than those obtained with the fixed value of 40.7×10^{-4} cm^{-1}.[6] Also for the imidazole species, the predictions of eq 11 are very similar to the experimental values and significantly better than those possible with the equation found previously through DFT methods.[14] It is worth noticing that there is good agreement between A_z^{calcd} and A_z^{exptl} for [VO(bmida)(H_2O)], where an equatorial position is occupied by a benzimidazole rather than a simple imidazole ligand,[34] suggesting that our discussion is generally valid and can be applicable either to pyridine or to imidazole derivatives.

A particularly interesting application of this work is to the complexes $[VO(SalGly)(pyr)_2]$ and [VO(Sal-L-Ala)(bipy)].[26] In the first structure, the equatorial pyridine coordinated to the $V^{IV}O^{2+}$ ion is almost perpendicular to the V=O bond ($\theta = 86.2°$); in the second one, the contemporaneous coordination of two nitrogens of 2,2′-bipyridine results in a parallel arrangement of the two aromatic rings ($\theta = 2.1°$). Since the other three equatorial donors are the same (Table 3), the decrease of A_z can be attributed solely to a different contribution of the pyridine nitrogen, that in turn depends on the different orientations of the two aromatic rings with respect to the V=O group. The different contributions to A_z calculated through eq 9, 44.0 for [VO(SalGly)($pyr)_2$] and 40.4×10^{-4} cm^{-1} for [VO(Sal-L-Ala)(bipy)], exactly correspond to the difference of 3.5×10^{-4} cm^{-1} in the experimentally observed A_z. Interestingly, a value of 163.3×10^{-4} cm^{-1} is expected for both of the complexes for a constant contribution of pyridine nitrogen.[6]

As above-mentioned, the theoretical explanation of the orientation dependence of the ^{51}V A_z value in $V^{IV}O^{2+}$ imidazole complexes is the decrease in the overlap between the π orbital of the aromatic system and the vanadium d_{xy} orbital bearing the unpaired electron, when the imidazole ring is rotated from a parallel ($\theta = 0°$) to perpendicular ($\theta = 90°$) orientation relative to the V=O bond. Such a rotation results in an increase in the metal character of the singly occupied molecular orbital (SOMO) and in a concomitant increase of the A_z value.[8]

DFT calculations reported here confirm this hypothesis. The list of the values of orbital contributions to the SOMO for $[VO(pyr)(H_2O)_3]^{2+}$ and $[VO(imid)(H_2O)_3]^{2+}$ species from $\theta = 0$ to $\theta = 90°$ is reported in Table 4, whereas the data for the whole range of θ values studied (0−180°) are presented in Tables S5 and S6 of the Supporting Information.

The calculated percentages of vanadium d and ligand π orbital contributions to the SOMO as a function of the dihedral angle θ are plotted in Figure 5. In the θ range 0−90°, as the vanadium d percentage increases, the aromatic π orbital contribution decreases following a

(35) Allen, F. H.; Kennard, O. *Chem. Des. Autom. News* **1993**, *8*, 31–37.

Table 4. Calculated Percentages of Orbital Contribution to the SOMO for $[VO(pyr)(H_2O)_3]^{2+}$ and $[VO(imid)(H_2O)_3]^{2+}$ Complexes

	$[VO(pyr)(H_2O)_3]^{2+}$					$[VO(imid)(H_2O)_3]^{2+}$				
dihedral angle	d vanadium orbitals	pyridine orbitals	π pyridine orbitals	O(oxo) + water	spin density	d vanadium orbitals	imidazole orbitals	π imidazole orbitals	O(oxo) + water	spin density
0°	79.78	15.90	10.86	4.32	1.167	86.78	8.61	8.23	4.61	1.159
10°	79.82	15.80	10.71	4.37	1.168	86.78	8.56	8.04	4.63	1.160
20°	80.05	15.45	10.50	4.46	1.169	86.95	8.37	7.66	4.67	1.162
30°	80.56	14.73	9.98	4.64	1.172	87.26	8.00	7.18	4.73	1.165
40°	81.50	13.59	9.57	4.81	1.176	87.76	7.40	6.41	4.81	1.169
50°	82.94	11.93	8.93	5.02	1.180	88.48	6.60	4.93	4.89	1.174
60°	85.01	9.75	7.34	5.14	1.183	89.40	5.56	3.07	5.01	1.178
70°	88.89	6.14	3.96	4.93	1.186	91.29	3.76	2.01	4.92	1.181
80°	90.04	3.34	0.84	6.55	1.188	92.40	2.71	1.13	4.83	1.183
90°	90.80	2.60	0.20	6.55	1.189	93.15	2.28	1.01	4.54	1.183

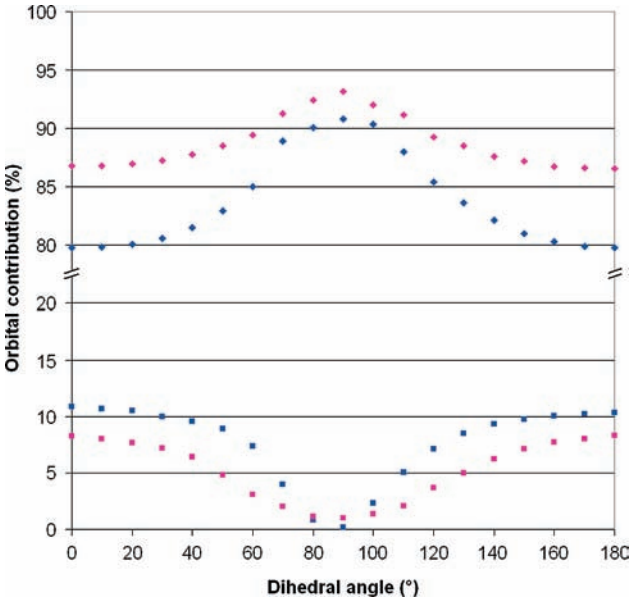

Figure 5. Calculated percentages of vanadium d (rhombi) and aromatic π (squares) orbitals contributions to the SOMO for $[VO(pyr)(H_2O)_3]^{2+}$ (blue) and $[VO(imid)(H_2O)_3]^{2+}$ (pink) complexes as a function of the dihedral angle θ.

sinusoidal dependence. This trend follows the observed variation in A_z and supports the prior explanation for this phenomenom.[8,14] It is worth noticing, however, that not only the coordinated nitrogen takes part in the delocalization of the unpaired electron[14] but also the entire π system of the pyridine or imidazole rings. This conclusion is observable in Figure 6, where the SOMO of $[VO(pyr)(H_2O)_3]^{2+}$ when $\theta = 0°$ and $\theta = 70°$ is represented. As demonstrated by the resemblance of eqs 9 and 11, the participations of pyridine and imidazole π orbitals in the SOMO are comparable.

It can be highlighted that both O(oxo) and water molecules contribute to the SOMO composition, with a total percentage variable from 4.3 to 6.6% for $[VO(pyr)(H_2O)_3]^{2+}$ and from 4.6 to 5.1% for $[VO(imid)(H_2O)_3]^{2+}$ (Table 4 and Tables S5 and S6 of the Supporting Information).

Finally, DFT calculations indicate that, as expected, the vanadium d orbital, which mainly contributes to the SOMO, is the d_{xy} orbital; however, this contribution is not exclusive, as the d_{xz} orbital also participates, with a percentage in the range 0−12% for $[VO(imid)(H_2O)_3]^{2+}$ but as high as 39% for $[VO(pyr)(H_2O)_3]^{2+}$ when the aromatic ring

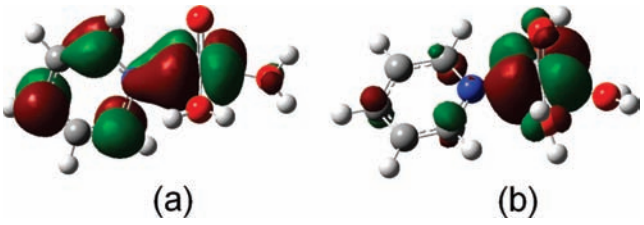

Figure 6. Representation of the SOMO for $[VO(pyr)(H_2O)_3]^{2+}$: (a) $\theta = 0°$ and (b) $\theta = 70°$.

is parallel to the V=O bond (Tables S5 and S6 of the Supporting Information).

Conclusions and Outlook

DFT calculations on a model $V^{IV}O^{2+}$ pyridine complex, $[VO(pyr)(H_2O)_3]^{2+}$, were used to investigate the orientation dependence of the ^{51}V hyperfine coupling constants as a function of the dihedral angle θ between the V=O and the N−C aromatic bonds. A similar procedure allows for reinvestigating such a dependence also for $V^{IV}O^{2+}$ imidazole species. The results show that both the A_{iso} and A_z vary according to the functional relationship $A + B \times \sin(2\theta - 90)$, with different values of the constants A and B, as predicted by Pecoraro and co-workers for $V^{IV}O^{2+}$ complexes formed by imidazole derivatives.[8]

The orientation dependence of A_z on θ was explained, as previously proposed,[8,14] with the change in the calculated percentage composition of the SOMO for the pyridine and imidazole $V^{IV}O^{2+}$ complexes. In particular, it was found that the increase of the absolute value of A_z when the dihedral angle θ between the V=O and N_{pyr}−C or N_{imid}−C bonds varies from a parallel to a perpendicular corresponds to an increase of the d vanadium orbital contribution (depending mainly on the d_{xy} orbital) and to a decrease of the π aromatic system participation in the SOMO.

The use of the half-and-half hybrid BHandHLYP functional,[15] instead of simple hybrid BP86,[14] results in a better prediction of the A_z values. Our calculations, with respect to that of Saladino and Larsen,[14] do not simply reproduce the range covered by A_z(imid) but are also able to predict its mean value.[8]

The applicability of these results to the benzimidazole derivatives[34] further demonstrates that the angular dependence of the A_z value of $V^{IV}O^{2+}$ species follows the conclusions reached by Pecoraro and co-workers.[8] This conclusion suggests that, in cases where V=O is bound to other important biomolecules such as tryptophan or to

nucleobases such as adenine and guanine, a similar dependence should occur. As V=O can be used as a probe to examine metal binding sites in DNA and RNA,[36] this orientation dependence needs to be considered when the structures of these vanadium biomolecules are evaluated.[37] It should be emphasized that, while the trend of variation in A_z for nucleobase orientation should generally follow the rules described herein for imidazole and pyridine complexes, the absolute magnitude of the effect is still unknown. We are now in a position to assess these values; therefore, we plan to perform further work, where the contribution to A_z of nitrogen donors belonging to nucleobases such as adenine and guanine will be studied. A similar effect may also be seen in vanadyl proteins for coordination by tryptophan. It could be interesting to evaluate if also A_z of species containing non-aromatic nitrogen donors show an angular dependence, or if this effect is limited to the aromatic amines.

Thus, we are close to having a generalizable method for not only assessing the first coordination sphere ligands bound to vanadium in a small molecule model or in a larger biomolecule but also for the ability to deduce variations in the first coordination sphere orientation of such complexes.

Supporting Information Available: Figures with the optimized structures and the variation of A_z and A_{iso} as a function of the dihedral angle θ for $[VO(pyr)(H_2O)_3]^{2+}$ and $[VO(imid)(H_2O)_3]^{2+}$; tables with the calculated EPR parameters, with the experimental and calculated A_z values for $V^{IV}O^{2+}$ pyridine and imidazole complexes reported in the literature and with the orbital contribution to the SOMO for $[VO(pyr)(H_2O)_3]^{2+}$ and $[VO(imid)(H_2O)_3]^{2+}$. This material is available free of charge via the Internet at http://pubs.acs.org.

(36) Snipes, W. W.; Gordy, W. *J. Chem. Phys.* **1964**, *41*, 3661–3662.
(37) Makinen, M. W.; Mustafi, D. In *Metal Ions in Biological Systems*; Sigel, A., Sigel, H., Eds.; Marcel Dekker: New York, 1995; Vol *31*, pp 89−127 and references therein.